

# Spinel $\text{LiNi}_{0.5}\text{Mn}_{1.5}\text{O}_4$ and its derivatives as cathodes for high-voltage Li-ion batteries

G. Q. Liu · L. Wen · Y. M. Liu

Received: 9 December 2009 / Revised: 19 March 2010 / Accepted: 23 March 2010 / Published online: 16 April 2010  
© Springer-Verlag 2010

**Abstract** The spinel material  $\text{LiNi}_{0.5}\text{Mn}_{1.5}\text{O}_4$  displays a remarkable property of high charge/discharge voltage plateau at around 4.7 V. It is a promising cathode material for new-generation lithium-ion batteries with high voltage. Recently, a lot of researches related to this material have been carried out. In this review we present a summary of these researches, including the structure, the mechanism of high voltage, and the latest developments in improving its electrochemical properties like rate ability and cycle performance at elevated temperature, etc. Doping element and synthesizing nanoscale material are effective ways to improve its rate ability. The novel battery systems, like  $\text{LiNi}_{0.5}\text{Mn}_{1.5}\text{O}_4/\text{Li}_5\text{Ti}_4\text{O}_{12}$  with good electrochemical properties, are also in progress.

**Keywords** Inorganic compounds · Oxides · Chemical synthesis · Electrochemical properties

## Introduction

Lithium-ion batteries (LIB) have been widely used in consumer electronics now. Compared to other batteries, they have many advantages such as the best energy-to-weight ratios, no memory effect, and a slow loss of charge when not in use [1, 2]. In addition to uses for consumer electronics, lithium-ion batteries are growing in popularity for defense,

automotive, and aerospace applications due to their high energy density. The battery property depends upon three important factors such as nature of cathode, anode, and the types of electrolyte used. Among the cathode materials,  $\text{LiCoO}_2$  has been used since the invention of LIB [3], while  $\text{LiMn}_2\text{O}_4$  and  $\text{LiFePO}_4$  are considered as promising ones due to less toxicity, low cost, more safety, and good electrochemical properties [4, 5]. However, both  $\text{LiMn}_2\text{O}_4$  and  $\text{LiFePO}_4$  have limited energy density because of their low capacity or operating voltage. One way to improve the energy and power densities is to increase the operating voltage. Tables 1 and 2 gives a comparison of main properties between these cathode materials [6–8]. The characteristic of voltage vs. capacity for several positive electrode materials is illustrated in Fig. 1 [9].

It can be seen that the most remarkable property of spinel  $\text{LiNi}_{0.5}\text{Mn}_{1.5}\text{O}_4$  is its discharge voltage plateau at around 4.7 V which is the highest one among these materials. In some cases, the demanded high voltage will need fewer high-voltage batteries in series than common batteries. It is easier to control these fewer batteries. For example, hundreds of ordinary lithium-ion batteries are needed to meet the specification of electric vehicle (EV) in the state of start-up, accelerate, and climb-up [10]. If the 5-V batteries are employed, the amount of batteries used for EV can decrease greatly.

Besides the high voltage, the doped spinel can also present a large discharge capacity of 150–160  $\text{mAh g}^{-1}$  and fairly good cyclability at around 3 V. For the doped spinels, during lithium insertion, the initial Ni–Mn ordering disappears and Ni-rich and Ni-poor domains form, leading to two Jahn-Teller-distorted tetragonal phases with different Ni–Mn ratios. The newly formed tetragonal phase with a right Ni–Mn ratio has a higher cyclability and a higher capacity [11–14].

G. Q. Liu (✉) · Y. M. Liu  
School of Material and Metallurgy, Northeastern University,  
Shenyang 110004, China  
e-mail: liugq@smm.neu.edu.cn

L. Wen  
Chinese Academy of Sciences, Institute of Metal Research,  
Shenyang National Laboratory for Materials Science,  
Shenyang 110016, China

**Table 1** Comparison of cathode materials for lithium-ion batteries [6–8]

Cathode material	Average voltage	Gravimetric capacity	Gravimetric energy
LiCoO <sub>2</sub>	3.7 V	140 mAh g <sup>-1</sup>	0.518 kWh kg <sup>-1</sup>
LiMn <sub>2</sub> O <sub>4</sub>	4.0 V	110 mAh g <sup>-1</sup>	0.440 kWh kg <sup>-1</sup>
LiNiO <sub>2</sub>	3.5 V	180 mAh g <sup>-1</sup>	0.630 kWh kg <sup>-1</sup>
LiFePO <sub>4</sub>	3.3 V	150 mAh g <sup>-1</sup>	0.495 kWh kg <sup>-1</sup>
Li <sub>2</sub> FePO <sub>4</sub> F	3.6 V	115 mAh g <sup>-1</sup>	0.414 kWh kg <sup>-1</sup>
LiCo <sub>1/3</sub> Ni <sub>1/3</sub> Mn <sub>1/3</sub> O <sub>2</sub>	3.6 V	160 mAh g <sup>-1</sup>	0.576 kWh kg <sup>-1</sup>
Li(Li <sub>a</sub> Co <sub>x</sub> Ni <sub>y</sub> Mn <sub>z</sub> )O <sub>2</sub>	4.2 V	220 mAh g <sup>-1</sup>	0.920 kWh kg <sup>-1</sup>
LiNi <sub>0.5</sub> Mn <sub>1.5</sub> O <sub>4</sub>	4.7 V	146 mAh g <sup>-1</sup>	0.686 kWh kg <sup>-1</sup>

Although other cation-substituted spinel oxides LiMn<sub>2-x</sub>M<sub>x</sub>O<sub>4</sub> (M=Cr, Co, Fe, and Cu) can also deliver capacity at around 5 V, the Ni Substituted spinel LiNi<sub>0.5</sub>Mn<sub>1.5</sub>O<sub>4</sub> is one of the most promising high-voltage materials for Li-ion battery application. The main problem about these high-voltage spinels is a possible corrosion reaction between the cathode surface and the electrolyte at the high voltage of 5 V. Recent researches demonstrate that the electrochemical properties of LiNi<sub>0.5</sub>Mn<sub>1.5</sub>O<sub>4</sub> are getting better and better.

This review sums up some important researches related to this spinel, including synthesizing method, nano-sized LiNi<sub>0.5</sub>Mn<sub>1.5</sub>O<sub>4</sub> spinels, doping element, coating on surface, analyzing mechanism of high voltage, fabricating advanced Li-ion batteries, electrochemical properties at elevated temperature, and comparing two kinds structure of primitive simple cubic structure (*P4<sub>3</sub>32*) and face-centered spinel (*Fd3m*). The latest research progresses which improve the electrochemical properties of LiNi<sub>0.5</sub>Mn<sub>1.5</sub>O<sub>4</sub> such as rate capability and cyclic performance are presented.

## Research progresses

Primitive simple cubic structure (*P4<sub>3</sub>32*) and face-centered spinel (*Fd3m*)

LiNi<sub>0.5</sub>Mn<sub>1.5</sub>O<sub>4</sub> has two possible structures of face-centered spinel (*Fd3m*) and primitive simple cubic crystal (*P4<sub>3</sub>32*). For

LiNi<sub>0.5</sub>Mn<sub>1.5</sub>O<sub>4</sub> with a face-centered structure (*Fd3m*), the lithium ions are located in the 8a sites of the structure, the manganese and nickel ions are randomly distributed in the 16d sites. The oxygen ions which are cubic-close-packed occupy the 32e positions. For LiNi<sub>0.5</sub>Mn<sub>1.5</sub>O<sub>4</sub> (*P4<sub>3</sub>32*) with a primitive simple cubic structure, the manganese ions are distributed in 12d sites, and nickel ions in 4a sites. The oxygen ions occupy the 24e and 8c positions, while the lithium ions are located in the 8c sites. In this case, the Ni and Mn ions are ordered regularly [14–16]. Whether LiNi<sub>0.5</sub>Mn<sub>1.5</sub>O<sub>4</sub> has a structure of face-centered spinel (*Fd3m*) or primitive simple cubic (*P4<sub>3</sub>32*) depends on its synthetic routes. In synthesizing LiNi<sub>0.5</sub>Mn<sub>1.5</sub>O<sub>4</sub>, annealing process at 700 °C after calcination led to the ordering of Ni and Mn ions, making it transformed from face-centered spinel (*Fd3m*) to primitive cubic crystal (*P4<sub>3</sub>32*). LiNi<sub>0.5</sub>Mn<sub>1.5</sub>O<sub>4</sub> (*Fd3m*) exhibited better cycling performance than LiNi<sub>0.5</sub>Mn<sub>1.5</sub>O<sub>4</sub> (*P4<sub>3</sub>32*) at high rates [17]. Schematic drawing of the structures of LiNi<sub>0.5</sub>Mn<sub>1.5</sub>O<sub>4</sub> is shown in Fig. 2 [18].

LiNi<sub>0.5</sub>Mn<sub>1.5</sub>O<sub>4</sub> (*P4<sub>3</sub>32*) showed poorer electrochemical properties than did the LiNi<sub>0.5</sub>Mn<sub>1.5</sub>O<sub>4</sub> (*Fd3m*), which mainly due to the structural transformation during cycling. The face-centered spinel (*Fd3m*) is more promising to become cathode material.

Mechanism of high voltage and insertion/deinsertion

Based on the results obtained with the systems LiMn<sub>2-y</sub>Ni<sub>y</sub>O<sub>4</sub> and LiCr<sub>y</sub>Mn<sub>2-y</sub>O<sub>4</sub>, Dahn and Sigala [19, 20] previously

**Table 2** Comparison of cathode materials for lithium-ion batteries [6–8]

Cathode	LiFePO <sub>4</sub>	LiCoO <sub>2</sub>	LiMn <sub>2</sub> O <sub>4</sub>	LiNi <sub>0.5</sub> Mn <sub>1.5</sub> O <sub>4</sub>
Material group	Olivine	Layered	Spinel	Spinel
Safety	Safest	Not stable	Acceptable	Acceptable
Environmental concern	Most enviro-friendly	Very dangerous	Enviro-friendly	Enviro-friendly
Cost	Most economic	High	Acceptable	Acceptable
Cycle performance	Best/excellent	Acceptable	Acceptable	Acceptable
Temperature range	Excellent (-20–70 °C)	Decay beyond (-20–55 °C)	Decay extremely fast over 50 °C	Good (0–55 °C)

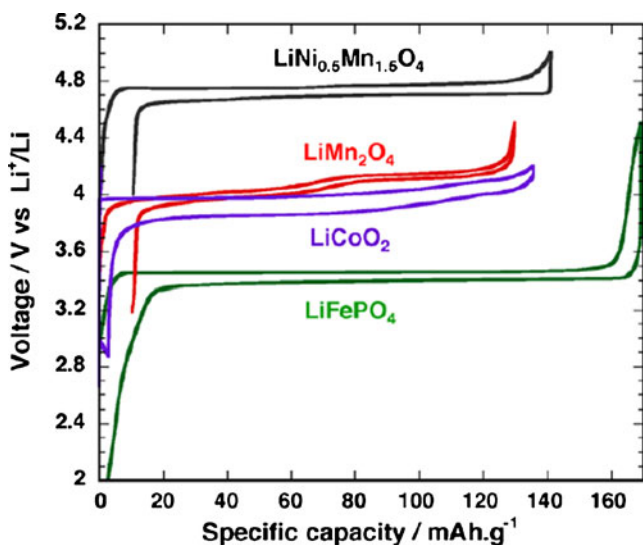
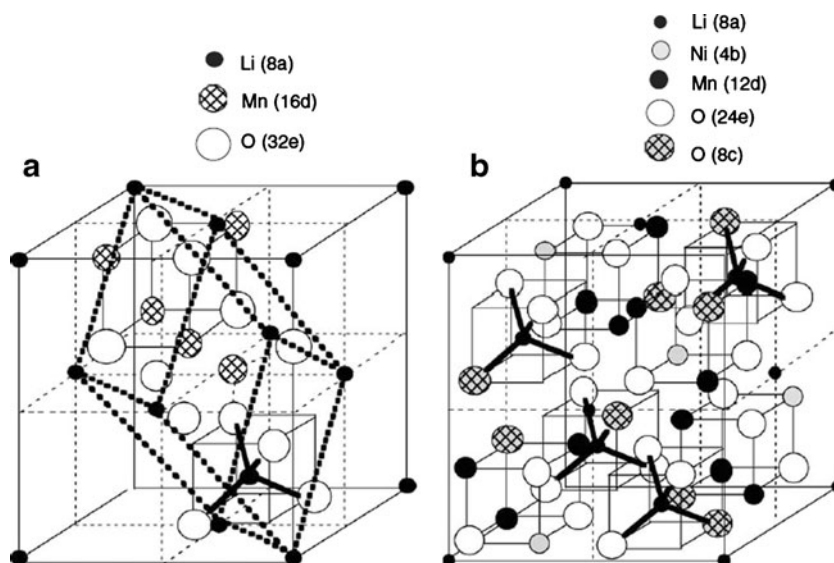


**Fig. 1** Comparison of several positive electrode materials (voltage vs. capacity, 20 °C, C/5 rate) [9]

pointed out that the high voltage originated from the oxidation of nickel and chromium ion. The 4.1 V plateau was related to the oxidation of  $\text{Mn}^{3+}$  to  $\text{Mn}^{4+}$  and the 4.7 V plateau to the oxidation of  $\text{Ni}^{2+}$  to  $\text{Ni}^{4+}$ . The oxidation of chromium ion could bring about a high voltage of 4.9 V. Yang [21] suggested that a significant amount of  $\text{Mn}^{4+}$  ion in the spinel framework was essential for electrochemical reaction to occur at around 5 V. His view was supported by Kawai [22] who argued that manganese-containing octahedra were necessary to impart high voltage capacity because manganese-free spinel oxides, such as  $\text{Li}_2\text{NiGe}_3\text{O}_8$ , did not show any capacity above 4.5 V. The influence of doping metals including  $\text{M}=\text{Cu}$  [23–25],  $\text{Co}$  [26],  $\text{Cr}$  [27–30],  $\text{Fe}$  [31–33],  $\text{Al}$  [34, 35], and  $\text{Zn}$  [36] on properties of

**Fig. 2** Schematic drawing of the structures of  $\text{LiNi}_{0.5}\text{Mn}_{1.5}\text{O}_4$  spinel lattice: **a** face-centered spinel ( $Fd\bar{3}m$ ), **b** primitive simple cubic ( $P4_332$ ) [18]



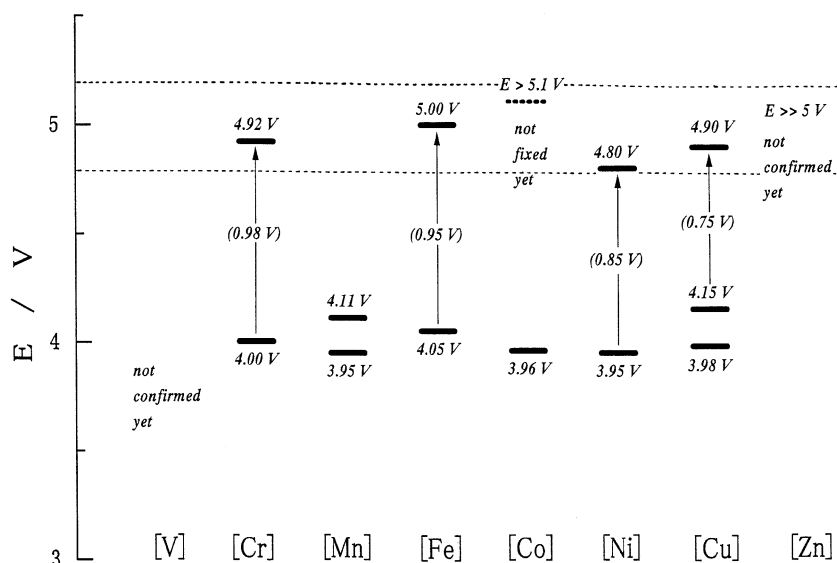
$\text{LiM}_{0.5}\text{Mn}_{1.5}\text{O}_4$  have been investigated. Compared to these materials, Ni-doped compound  $\text{LiM}_{0.5}\text{Mn}_{1.5}\text{O}_4$  displays higher capacity and better cycle ability. For spinel  $\text{LiNi}_{0.5}\text{Mn}_{1.5}\text{O}_4$ , there is a capacity occurring at 4.6–4.7 V, which can be attributed to a two electron process,  $\text{Ni}^{2+}/\text{Ni}^{4+}$ . While in the 4-V region, the electrode sometimes shows some minor redox behavior, related to the  $\text{Mn}^{3+}/\text{Mn}^{4+}$  couple. When there are more  $\text{Mn}^{4+}$  and  $\text{Ni}^{2+}$  in  $\text{LiNi}_{0.5}\text{Mn}_{1.5}\text{O}_4$ , then the corresponding capacity at 4 V will be less and that at 5 V will be large, and vice versa [37].

Gao [38] put forward an explanation for the origin of high voltage. As an electron is removed from  $\text{Mn}^{3+}$ , it is removed from  $\text{Mn } e_g (\uparrow)$  which has an electron binding energy at around 1.5–1.6 eV, and this is on the 4.1 V plateau. When there are no more electrons left on  $\text{Mn } e_g (\uparrow)$  (all Mn are  $\text{Mn}^{4+}$  now), electrons are removed from  $\text{Ni } e_g (\uparrow\downarrow)$  which has an electron binding energy of about 2.1 eV, and the voltage plateau moves up to 4.7 V because of the increased energy needed to remove electrons.

Ohzuku [39] investigated the redox potentials for  $\text{LiM}_{0.5}\text{Mn}_{1.5}\text{O}_4$  ( $\text{M}$ : 3d-transition metal). As shown in Fig. 3, the chromium, iron, cobalt, nickel, or copper-containing sample exhibited common solid-state redox potentials at  $5.0 \pm 0.2$  V in addition to  $4.0 \pm 0.1$  V vs.  $\text{Li}^+/\text{Li}$ .

Terada [40] studied the mechanism of the oxidation reaction during Li deintercalation by measuring the in situ XAFS spectra of  $\text{Li}_{1-x}(\text{Mn},\text{M})_2\text{O}_4$  ( $\text{M}=\text{Cr}, \text{Co}, \text{Ni}$ ). It is found from the Ni K-edge XAFS analysis that Ni in  $\text{Li}_{1-x}\text{Mn}_{1.69}\text{Ni}_{0.31}\text{O}_4$  experiences three distinct valence states with during Li deintercalation,  $\text{Ni}^{2+}$ ,  $\text{Ni}^{3+}$ , and  $\text{Ni}^{4+}$ . The X-ray absorption near-edge structures (XANES) of Mn and M show that the high voltage ( $\sim 5$  V) in the cathode materials of a Li secondary battery is due to the oxidation of  $\text{M}^{3+}$  to  $\text{M}^{4+}$  ( $\text{M}=\text{Cr}, \text{Co}$ ), and  $\text{M}^{2+}$  to  $\text{M}^{4+}$  ( $\text{M}=\text{Ni}$ ). The origin of

**Fig. 3** Levels of solid-state redox potentials for  $\text{LiMe}_{0.5}\text{Mn}_{1.5}\text{O}_4$  (Me=Cr, Fe, Co, Ni, Cu) [39]



the low voltage (3.9–4.3 V) is ascribed to the oxidation of  $\text{Mn}^{3+}$  to  $\text{Mn}^{4+}$ .

Ariyoshi [41] reported that the reaction at ca. 4.7 V occurred via formation of two cubic phases, i.e., **b**  $[\text{Ni}_{1/2}\text{Mn}_{3/2}]\text{O}_4$  was reduced to  $\text{Li}[\text{Ni}_{1/2}\text{Mn}_{3/2}]\text{O}_4$  via  $\text{Li}_{1/2}[\text{Ni}_{1/2}\text{Mn}_{3/2}]\text{O}_4$  (**b** represents lithium vacancy). The flat voltage at ca. 4.7 V consisted of two voltages of 4.718 and 4.739 V. The reaction of  $\text{Li}[\text{Ni}_{1/2}\text{Mn}_{3/2}]\text{O}_4$  to  $\text{Li}_2[\text{Ni}_{1/2}\text{Mn}_{3/2}]\text{O}_4$  proceeded in a cubic/tetragonal two-phase reaction with the reversible potential of 2.795 V.

To sum up, for spinel  $\text{LiMe}_{0.5}\text{Mn}_{1.5}\text{O}_4$ , there are three main voltage plateaus at around 3, 4, and above 4.5 V. The 3 V plateau corresponds to a reaction of  $\text{Li}[\text{Ni}_{1/2}\text{Mn}_{3/2}]\text{O}_4$  to  $\text{Li}_2[\text{Ni}_{1/2}\text{Mn}_{3/2}]\text{O}_4$ , the 4 V plateau results from an oxidation/reduction of  $\text{Mn}^{4+}/\text{Mn}^{3+}$ , and the above 4.5 V plateau is attributed to an oxidation/reduction of the doping elements.

#### Synthesizing method

Solid-state reaction is a commonly used method to prepare electrode materials for lithium-ion batteries. It is simple and suitable for mass production. However, the solid-state reaction used commonly to prepare  $\text{LiNi}_{0.5}\text{Mn}_{1.5}\text{O}_4$  is not adequate to control the composition of Ni and Mn, and produces impurity in the form of nickel oxide. The capacity of  $\text{LiNi}_{0.5}\text{Mn}_{1.5}\text{O}_4$  prepared through solid-state reaction is only 120  $\text{mAh g}^{-1}$  [42]. Fang [43] prepared  $\text{LiNi}_{0.5}\text{Mn}_{1.5}\text{O}_4$  by an improved solid-state reaction. He used appropriate amounts of  $\text{Li}_2\text{CO}_3$ , NiO, and electrolytic  $\text{MnO}_2$  as reactants. After being thoroughly ball-milled, the mixed precursors were heated up to 900 °C, then directly cooled down to 600 °C and heated for 24 h in air. The heating and cooling rates were about 30 and 10 °C/min, respectively. The product could deliver 143  $\text{mAh g}^{-1}$  at 5/7 C and still

retained 141  $\text{mAh g}^{-1}$  after 30 cycles. Fang also synthesized  $\text{LiNi}_{0.5}\text{Mn}_{1.5}\text{O}_4$  using a one-step solid-state reaction at 600 °C in air. The prepared product delivered up to 138  $\text{mAh g}^{-1}$ , and the capacity retained 128  $\text{mAh g}^{-1}$  after 30 cycles [44]. Recently Chen employed a mechanical activated solid-state reaction from stoichiometric amount of  $\text{Ni}(\text{NO}_3)_2 \cdot 6\text{H}_2\text{O}$ ,  $\text{MnO}_2$ , and  $\text{Li}_2\text{CO}_3$  to prepare  $\text{LiNi}_{0.5}\text{Mn}_{1.5}\text{O}_4$ . Its reversible capacity was about 145  $\text{mAh g}^{-1}$  and remained 143  $\text{mAh g}^{-1}$  after 10 cycles [45]. Other solid-state reaction reports have also been reported [46–57].

In order to obtain high-purity spinel phase, various synthesis methods have been developed. These methods include co-precipitation method [58–61], polymer-pyrolysis method [62, 63], ultrasonic-assisted co-precipitation method [64, 65], sol-gel method [66–68], radiated polymer gel method [69], sucrose-aided combustion method [70], spray-drying method [71], emulsion-drying method [72], composite carbonate process [73], molten salt method (MSM) [74, 75], mechanochemical process [76], poly (methyl methacrylate)-assisted method [77] ultrasonic spray pyrolysis [78], polymer-assisted synthesis [79], combinational annealing method [21], pulsed laser deposition [80], electrophoretic deposition [81], spin-coating deposition [82], carbon combustion synthesis [83], soft combustion reaction method [84], pulsed laser deposition [85], spray-drying and post-annealing [86], rheological method [87], self-reaction method [88], internal combustion type spray pyrolysis [89, 90], a chloride-ammonia co-precipitation method [83], a novel carbon exo-templating method [91], flame type spray pyrolysis [92], self-combustion reaction [93], and so on.

Molten salt method is one of the simplest techniques for preparing ceramic materials including mixed oxides. It is based on the use of a salt with low melting point, such as

alkali chlorides, sulfates, carbonates, or hydroxides, as a reaction medium. The obtained product with no impurity usually can be obtained at relatively lower temperatures because diffusion rates between reaction components are high in the molten media. Kim [75] reported that a  $\text{LiNi}_{0.5}\text{Mn}_{1.5}\text{O}_4$  was synthesized by this molten salt method. The product delivered an initial discharge capacity of  $139 \text{ mAh g}^{-1}$ , and its capacity retention rate exceeded 99% after 50 cycles, as shown in Fig. 4. Although this product exhibited excellent cycle performance, it was tested at a low current rate. What performance it will show at high current rates is worth expecting of.

The electrochemical properties of spinel  $\text{LiNi}_{0.5}\text{Mn}_{1.5}\text{O}_4$  are affected by many factors like purity, component ratio, shape and size of product powders, and so on. States of product will be different due to employing different synthesis methods. Molten salt method is a new preparation method of inorganic material powders, and it has advantages of simple process, relative lower synthesizing temperature, and shorter synthesizing time. The products are usually with higher purity, non-segregation and accurate component ratio, and the shape and size of the product powders can be controlled by the MSM.

#### Electrochemical performance at elevated temperature

According to researches, the spinel  $\text{LiMn}_2\text{O}_4$  electrode in the 4-V regions suffered from a poor cycling behavior at 50–80 °C [94–96]. The Ni-doped material  $\text{LiNi}_{0.5}\text{Mn}_{1.5}\text{O}_4$  exhibited improved performance at elevated temperature. For example, Aurbach [97] studied the electrochemical properties of  $\text{LiNi}_{0.5}\text{Mn}_{1.5}\text{O}_4$  at 60 °C. The voltammograms showed that the resolution of the sets of anodic and cathodic peaks at 60 °C is better, indicating that the  $\text{LiNi}_{0.5}\text{Mn}_{1.5}\text{O}_4$  electrodes should conduct faster kinetics. The voltammograms result is shown in Fig. 5a. The cycle tests showed that there was a gradual decrease in the capacity in the temperature range around 25–60 °C, as illustrated in Fig. 5b. A “compensation mechanism” was

presented for this result. It expounded that the gradual decrease in the capacity was mostly due to sluggish kinetics and not to a pronounced degradation of the active mass. The capacity ‘losses’ upon charging at constant currents could be compensated for by charging at a constant high potential (4.9 V vs.  $\text{Li/Li}^+$ ). The measurement displays that spinel  $\text{LiNi}_{0.5}\text{Mn}_{1.5}\text{O}_4$  can deliver a capacity of about  $145 \text{ mAh g}^{-1}$  with good cycle performance at both 60 and 25 °C. However, the charge/discharge processes were carried out at a low current rate of  $C/20$ , some tests at higher current rate should be conducted to investigate the performance of spinel  $\text{LiNi}_{0.5}\text{Mn}_{1.5}\text{O}_4$  at elevated temperature.

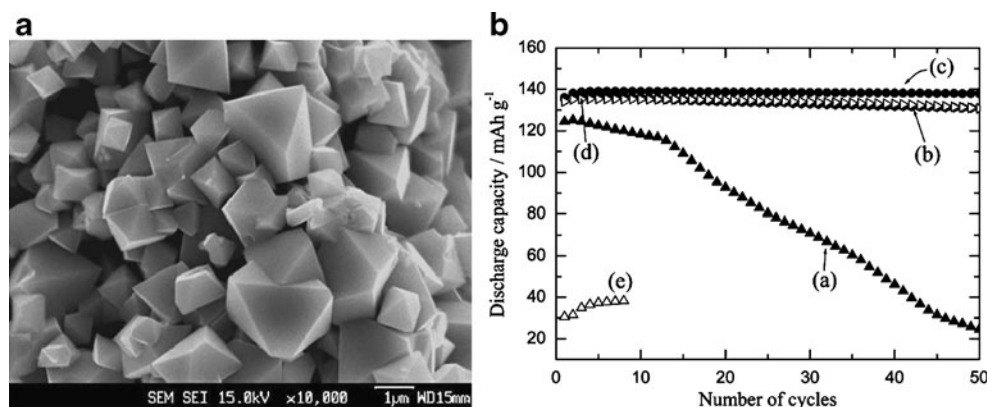
Considering electrolyte decomposition by water traces [98]:  $\text{LiPF}_6 + \text{H}_2\text{O} \rightarrow \text{POF}_3 + \text{LiF} + 2\text{HF}$ . The HF could attack cathode material to make transitional metal to dissolve. Thus, a coating layer on the surface of electrode materials is necessary for the electrode to maintain good cycle performances. Arrebola [99] and Sun [100] studied the effect of coating ZnO on  $\text{LiNi}_{0.5}\text{Mn}_{1.5}\text{O}_4$  spinel in the temperature range of 50–55 °C. Some positive effects of coating ZnO have been obtained, as can be seen in Fig. 5c.

It is noticed that Fig. 5b and c have presented different results related to cycle performance of  $\text{LiNi}_{0.5}\text{Mn}_{1.5}\text{O}_4$  at elevated temperature. The reason for this difference is that the latter was carried out in an electrolyte containing 25 ppm of HF content and the current rates were also different. So when there is HF content in electrolyte, good electrochemical performance can be obtained by coating protective layer on the surface of Ni-doped material  $\text{LiNi}_{0.5}\text{Mn}_{1.5}\text{O}_4$ . Besides ZnO layer, other materials which can resist attack from HF and have good conductivity can also be employed.

#### Nano-sized $\text{LiNi}_{0.5}\text{Mn}_{1.5}\text{O}_4$ spinels

Nanostructure materials have both advantages and disadvantages for lithium batteries. The advantages include short path lengths for  $\text{Li}^+$  transport, short path lengths for electronic transport, higher electrode/electrolyte contact

**Fig. 4** **a** SEM image of the  $\text{LiNi}_{0.5}\text{Mn}_{1.5}\text{O}_4$  powders synthesized using molten salt at 900 °C for 3 h; **b** the electrochemical cycling performances of the  $\text{Li/LiNi}_{0.5}\text{Mn}_{1.5}\text{O}_4$  cells at a constant current density of  $20 \text{ mA g}^{-1}$  ( $0.2 \text{ mA cm}^{-2}$ ) prepared at various calcination temperatures with the same amount of LiCl salt: (a) 700 °C; (b) 800 °C; (c) 900 °C; (d) 950 °C; and (e) 1,000 °C [75]



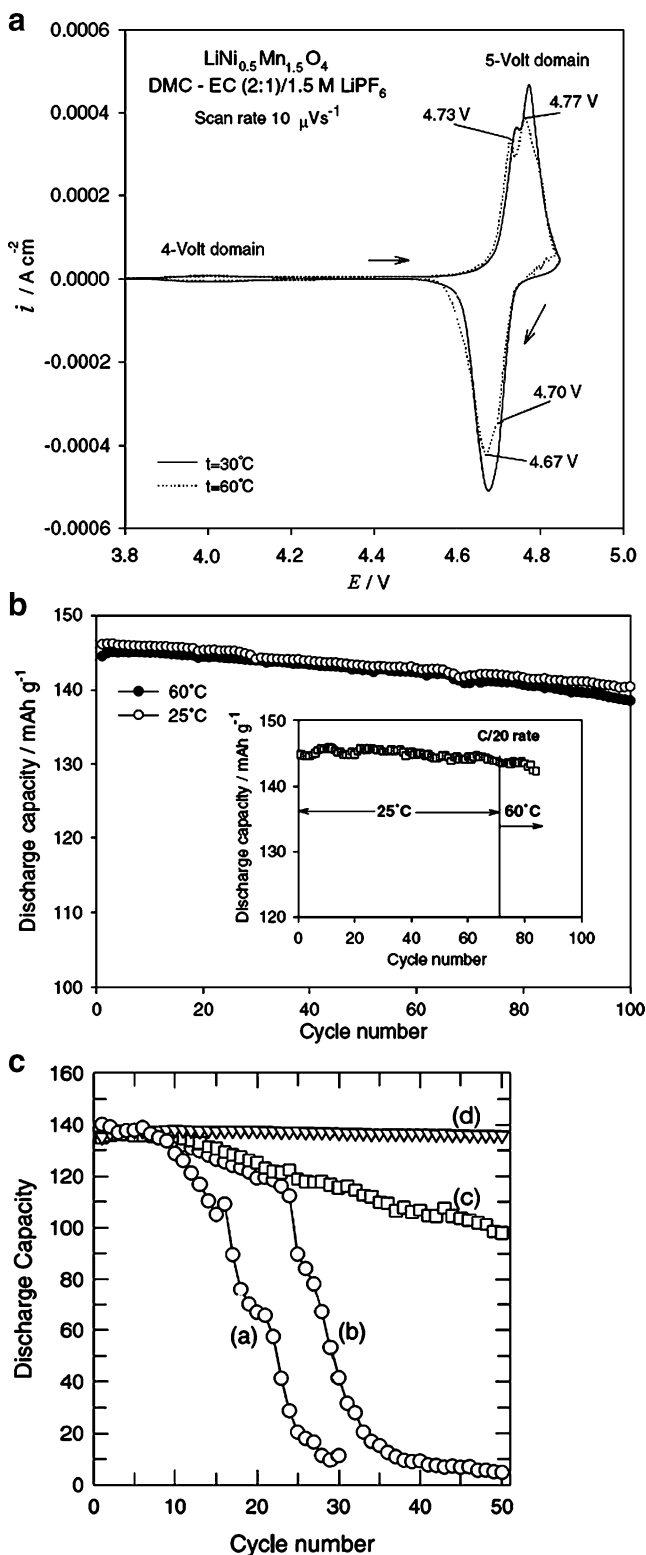


**Fig. 5** **a** Cyclic voltammograms of  $\text{LiNi}_{0.5}\text{Mn}_{1.5}\text{O}_4$  electrodes obtained at 25 and 60 °C coin cells, DMC–EC (2:1)/1.5 M  $\text{LiPF}_6$  solution [97]. **b** Comparison of cycling performance of  $\text{LiNi}_{0.5}\text{Mn}_{1.5}\text{O}_4$  electrodes at 25 and 60 °C. *Inset* discharge capacity as a function of cycle number of the  $\text{LiNi}_{0.5}\text{Mn}_{1.5}\text{O}_4$  electrode cycled first at 25 and then 60 °C (constant current mode, C/20) coin cells, DMC–EC (2:1)/1.5 M  $\text{LiPF}_6$  solution The potential range was 3.5–4.9 V [97]. **c** Specific discharge capacity of (a) the as-prepared  $\text{LiNi}_{0.5}\text{Mn}_{1.5}\text{O}_4$ , (b) 0.1%, (c) 0.5%, and (d) 1.5% ZnO-coated  $\text{LiNi}_{0.5}\text{Mn}_{1.5}\text{O}_4$  electrodes at 55 °C. The current rate was C/3 ( $0.4 \text{ mA cm}^{-2}$ ) [100]

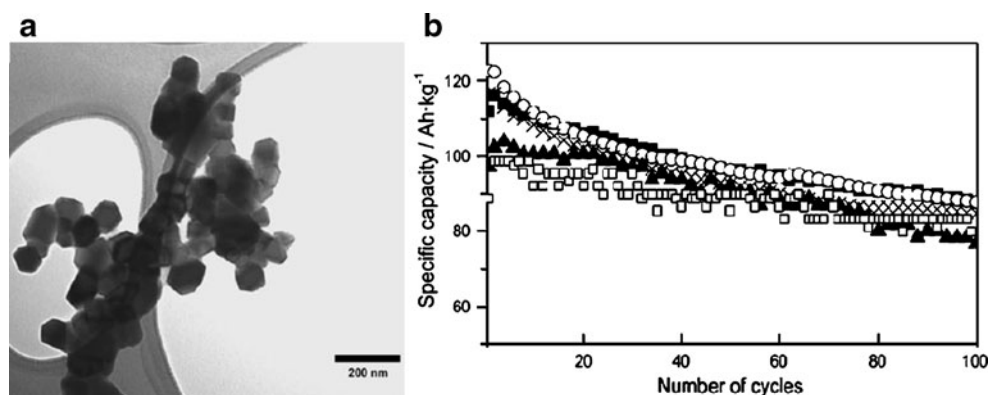
spinel have been reported [103–108]. In general, the nanometer particles exhibit a good performance at high rates due to the shortened diffusion paths, whereas at low rates the reactivity towards the electrolyte increases and the cell performance is lowered. Micrometric particles, which are less reactive towards the electrolyte, are a better choice for making electrodes under these latter conditions. Recently, some improvements have been achieved. Nanometer  $\text{LiNi}_{0.5}\text{Mn}_{1.5}\text{O}_4$  with good electrochemical performance over a wide range of rate capabilities by modifying the experimental synthetic conditions has also been reported. For example, Lafont [104] synthesized a nanomaterial  $\text{LiMg}_{0.05}\text{Ni}_{0.45}\text{Mn}_{1.5}\text{O}_4$  of about 50 nm in size with an ordered cubic spinel phase ( $\text{P4}_3\text{32}$ ) by auto-ignition method. It displayed good capacity retention of  $131 \text{ mAh g}^{-1}$  at C/10 and  $90 \text{ mAh g}^{-1}$  at 5 C. By using a template method, Arrebola [109] synthesized  $\text{LiNi}_{0.5}\text{Mn}_{1.5}\text{O}_4$  nanorods and nanoparticles using PEG (polyethyleneglycol) 800 as the sacrificial template. Highly crystalline nanometric  $\text{LiNi}_{0.5}\text{Mn}_{1.5}\text{O}_4$  of 70–80 nm was prepared at 800 °C. Its electrochemical properties were measured at different charge/discharge rates of C/4, 2 C, 4 C, 8 C, and 15 C. The capacity values were  $121 \text{ mAh g}^{-1}$  at 2 C and  $98 \text{ mAh g}^{-1}$  at 15 C, and faded slowly on cycling, as shown in Fig. 6a and b. The current rate of 15 C has been the highest rate tested for  $\text{LiNi}_{0.5}\text{Mn}_{1.5}\text{O}_4$  so far. It can be predicted that the capacity will continue to fade when cycling. So the capacity retention at high current rates needs further improvement for nanometric  $\text{LiNi}_{0.5}\text{Mn}_{1.5}\text{O}_4$ .

Besides particle sizes, particle morphology and crystallinity also play a role in properties of materials. Kunduraci [110] synthesized a three-dimensional mesoporous network structure with nano-size particles and high crystallinity. This morphology allows easy electrolyte penetration into pores and continuous interconnectivity of particles, yielding high power densities at fast discharges.

At present the electrode materials have reached their intrinsic limits, nanomaterials provide a new way to improve their properties. It is no doubt that nano-sized electrode materials including nano- $\text{LiNi}_{0.5}\text{Mn}_{1.5}\text{O}_4$  will gradually be applied in futur high-energy lithium-ion batteries. To realize the commercial application of nano-

area leading to higher charge/discharge rates, while the disadvantage include an increase in undesirable electrode/electrolyte reactions due to high surface area, leading to self-discharge, poor cycling, and calendar life [101, 102]. Some researches relative to nano-sized  $\text{LiNi}_{0.5}\text{Mn}_{1.5}\text{O}_4$

**Fig. 6 a** TEM images of the PEG 800 sample; **b** cycle performances of the PEG 800 sample charge/discharge rate: C/4 (filled square), 2 C (unfilled circle), 4 C (multiplication symbol), 8 C (filled triangle), and 15 C (unfilled square) [109]. The nano-sized spinel  $\text{LiNi}_{0.5}\text{Mn}_{1.5}\text{O}_4$  exhibits good capacity retention at high charge/discharge rate



materials, some technical obstacles such as undesirable electrode/electrolyte reactions due to high surface area, self-discharge, and poor calendar life and so on should be overcome.

#### Doping elements

The structural and electrochemical properties of the  $\text{LiNi}_{0.5}\text{Mn}_{1.5}\text{O}_4$  could also be affected by the substitution of other metal ions. Cation doping is considered to be an effective way to modify the intrinsic properties of electrode materials. It will be promising if proper cation doping can be used in spinel  $\text{LiNi}_{0.5}\text{Mn}_{1.5}\text{O}_4$  to further improve its electrical conductivity, favoring fast charge and discharge rate. So far, some researches related to elements have been reported, such as doping Al [21], Fe [111–113], Cu [114], Co [115, 116], Ti [117–119], Cr [120–124], Mg [125], Zn [126], and Ru [127]. These doping elements had different influences on improving the electrochemical properties of  $\text{LiNi}_{0.5}\text{Mn}_{1.5}\text{O}_4$ . According to previous reports [118], spinel  $\text{LiNi}_{0.5}\text{Mn}_{1.5}\text{O}_4$  doped with Ti could maintain good cycle performance though its rate capability was not greatly improved. Better electrochemical properties are obtained for compound  $\text{LiCr}_{0.1}\text{Ni}_{0.4}\text{Mn}_{1.5}\text{O}_4$  [123] and  $\text{LiMn}_{1.5}\text{Ni}_{0.42}\text{Fe}_{0.08}\text{O}_4$  [113]. The  $\text{LiCr}_{0.1}\text{Ni}_{0.4}\text{Mn}_{1.5}\text{O}_4$  could deliver capacities of 143, 118, and 111  $\text{mAh g}^{-1}$  at current densities of 1.0, 4.0, and 5.0  $\text{mA cm}^{-2}$  with excellent capacity retention, respectively. While the  $\text{LiMn}_{1.5}\text{Ni}_{0.42}\text{Fe}_{0.08}\text{O}_4$  delivered a capacity of 136  $\text{mAh g}^{-1}$  at C/6 rate with capacity retention of 100% in 100 cycles and a remarkably high capacity of 106  $\text{mAh g}^{-1}$  at 10 C rate. Until now the spinel  $\text{LiNi}_{0.5}\text{Mn}_{1.5}\text{O}_4$  with trace Ru doping has been reported to exhibit the best electrochemical properties, including rate capability and cyclic performance. Wang [127] reported that  $\text{Li}_{1.1}\text{Ni}_{0.35}\text{Ru}_{0.05}\text{Mn}_{1.5}\text{O}_4$  and  $\text{LiNi}_{0.4}\text{Ru}_{0.05}\text{Mn}_{1.5}\text{O}_4$  could deliver discharge capacities of 108 and 117  $\text{mAh g}^{-1}$  at 10 C between 3 and 5 V, respectively. At 10 C charge/discharge rate, they could maintain 91% and 84% of their initial capacities after 500 cycles, respectively, as shown in Fig. 7. The doped Ru could

make lattice constants enlarge and lithium ion locate at octahedral sites rather than tetrahedral site, which is in favor of Li insertion/deinsertion. However, although the amount of doped Ru is small, its effect is prominent. The mechanism of doping Ru needs further studying, and it will play an instructional role in choosing proper element to dope.

Besides cation doping, there are some researches relative to the substitution of the small amount of  $\text{F}^-$  for  $\text{O}^{2-}$  anion [128–130]. In crystal structure, for face-centered spinel ( $Fd3m$ ), it is assumed that  $\text{Li}^+$  ions occupy the tetrahedral sites (8a),  $\text{Ni}^{2+}$  and  $\text{Mn}^{4+}$  ions are randomly located at the octahedral sites (16d), and  $\text{O}^{2-}$  and  $\text{F}^-$  ions are located at the 32e sites. The doped compounds like  $\text{LiNi}_{0.5}\text{Mn}_{1.5}\text{O}_{4-x}\text{F}_x$  have less lattice parameter than compound  $\text{LiNi}_{0.5}\text{Mn}_{1.5}\text{O}_4$  because fluorine substitution changes the oxidation state of transition metal components and more  $\text{Mn}^{3+}$  ions with larger ionic radius ( $r=0.645 \text{ \AA}$ ) will replace partial  $\text{Mn}^{4+}$  ions ( $r=0.53 \text{ \AA}$ ) for electro-neutrality. The content of fluorine has influence on electrochemical properties of the doped compounds. On

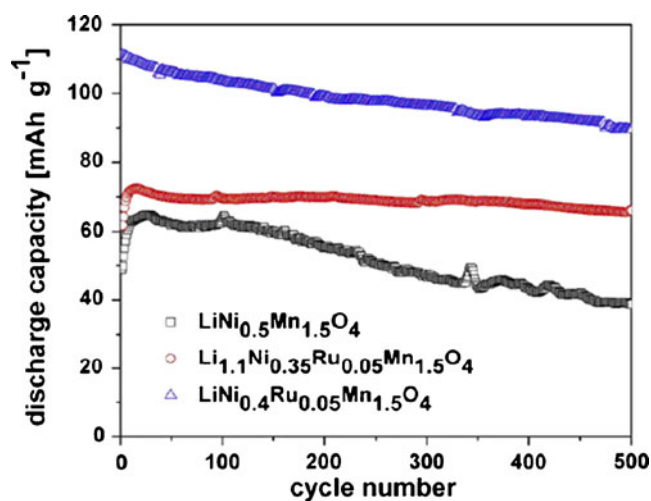


**Fig. 7** Capacity retention of  $\text{LiNi}_{0.5}\text{Mn}_{1.5}\text{O}_4$ ,  $\text{Li}_{1.1}\text{Ni}_{0.35}\text{Ru}_{0.05}\text{Mn}_{1.5}\text{O}_4$ , and  $\text{LiNi}_{0.4}\text{Ru}_{0.05}\text{Mn}_{1.5}\text{O}_4$  charged/discharged at 10 C [127]. The rate ability of  $\text{LiNi}_{0.5}\text{Mn}_{1.5}\text{O}_4$  is improved greatly by doping Ru

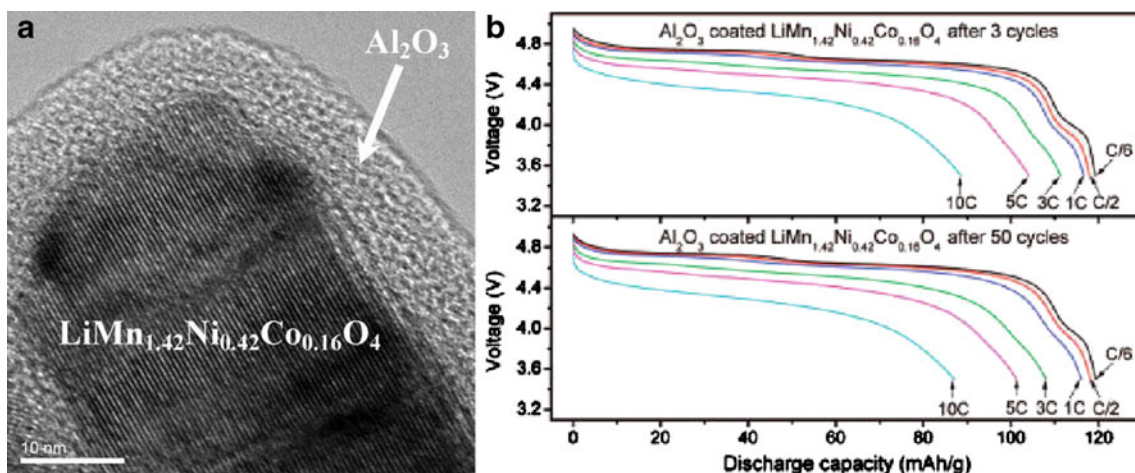


**Fig. 8** **a** High-resolution TEM images of 2 wt.%  $\text{Al}_2\text{O}_3$ -coated  $\text{LiMn}_{1.42}\text{Ni}_{0.42}\text{Co}_{0.16}\text{O}_4$ ; **b** discharge profiles illustrating the rate capabilities of bare and 2 wt.%  $\text{Al}_2\text{O}_3$ -coated  $\text{LiMn}_{1.42}\text{Ni}_{0.42}\text{Co}_{0.16}\text{O}_4$  after three and 50 cycles. Charge current density,  $20 \text{ mA g}^{-1}$  [133]

the one hand, strong Li–F bonding may hinder  $\text{Li}^+$  extraction, leading to a lower reversible capacity. On the other hand, fluorine doping makes spinel structure more stable due to the strong M–F bonding, which is favorable for the cyclic stability. According to the previous research report [130], the compound  $\text{LiNi}_{0.5}\text{Mn}_{1.5}\text{O}_{3.9}\text{F}_{0.1}$  displayed good electrochemical properties of an initial capacity of  $122 \text{ mAh g}^{-1}$  and a capacity retention of 91% after 100 cycles. In addition, Oh [128] studied the effect of fluorine substitution on thermal stability. He reported that the  $\text{Li}_{0.05}\text{Ni}_{0.5}\text{Mn}_{1.5}\text{O}_4$  electrode had an abrupt exothermic peak at around  $238.3 \text{ }^\circ\text{C}$  ( $1,958 \text{ J g}^{-1}$ ) when charged to 5.0 V. While  $\text{Li}_8\text{Ni}_{0.5}\text{Mn}_{1.5}\text{O}_{3.9}\text{F}_{0.1}$  electrodes exhibited smaller exothermic peaks at higher temperatures, i.e.,  $246.3 \text{ }^\circ\text{C}$  ( $464.2 \text{ J g}^{-1}$ ). So fluorine substitution is advantageous for the thermal stability of  $\text{Li}_8\text{Ni}_{0.5}\text{Mn}_{1.5}\text{O}_{4-x}\text{F}_x$  spinel.

Cation doping like doping Ru and Fe has achieved some encouraging results, improving the rate capability to a certain extent. Cation doping can improve conductivity, enlarge lattice constants and form stronger metal–O bond, etc., which are favorable for migrating lithium ion and maintaining stable crystal structure. Choosing appropriate element and amount, better electrochemical properties are expected to implement.

#### Surface modification

Although surface modifications applied to high-voltage material  $\text{LiNi}_{0.5}\text{Mn}_{1.5}\text{O}_4$  are much less than applied to those materials with layer structure like  $\text{LiCoO}_2$ , they are also effective ways to improve the properties of  $\text{LiNi}_{0.5}\text{Mn}_{1.5}\text{O}_4$ . The coating layer can protect cathode materials from attacking of HF in electrolyte. So far, surface modification of 5 V spinels has been mainly limited to  $\text{Bi}_2\text{O}_3$  [131],  $\text{Al}_2\text{O}_3$  [132, 133],  $\text{ZnO}$  [134–136],  $\text{Li}_3\text{PO}_4$  [137],  $\text{SiO}_2$

[138], Zn [139], and Au [140] which lead to better cycle performance and rate capability retention. However, the effect of coating the nanometric spinel  $\text{LiNi}_{0.5}\text{Mn}_{1.5}\text{O}_4$  with Ag on its rate capability was negative [141]. According to Liu [132],  $\text{Al}_2\text{O}_3$ -modified sample exhibited the best cyclability (99% capacity retention in 50 cycles) with a capacity of  $120 \text{ mAh g}^{-1}$ , while  $\text{Bi}_2\text{O}_3$ -coated sample exhibited the best rate capability. At a rate of 10 C, the  $\text{Bi}_2\text{O}_3$ -coated sample could deliver a capacity of about  $90 \text{ mAh g}^{-1}$  after 50 cycles. Liu [133] thought that  $\text{Al}_2\text{O}_3$  reacted with the surface of  $\text{LiMn}_{1.42}\text{Ni}_{0.42}\text{Co}_{0.16}\text{O}_4$  during the annealing process and formed  $\text{LiAlO}_2$  that exhibited good lithium-ion conductivity. Therefore, “ $\text{Al}_2\text{O}_3$ ” modification layer acts as both a protection shell and as a fast lithium-ion diffusion channel, rendering both excellent cycling performance and good rate capability for the

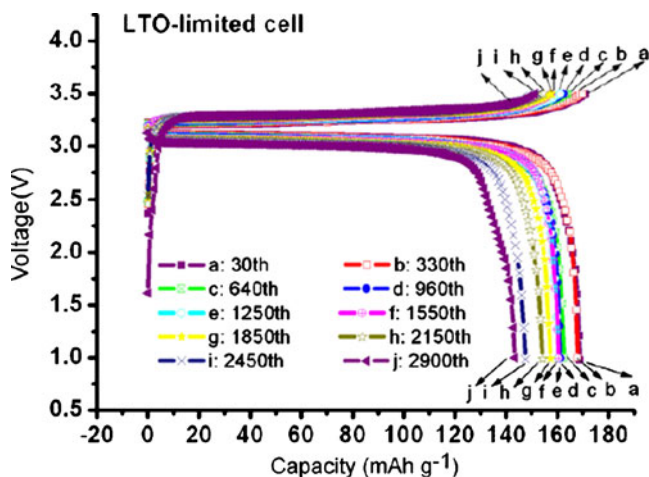


**Fig. 9** Results on the accelerated cycling tests of the LNMO/LTO cells with capacity limited by LTO anode. The test was carried out in the voltage range of 1.0–3.5 V at the current of  $0.2 \text{ mA cm}^{-2}$  [142]

$\text{Al}_2\text{O}_3$ -coated  $\text{LiMn}_{1.42}\text{Ni}_{0.42}\text{Co}_{0.16}\text{O}_4$ . Similarly,  $\text{Bi}_2\text{O}_3$  is reduced on the cathode surface during electrochemical cycling to metallic Bi, which is an electronic conductor, rendering both excellent rate capability and good cycling performance for the  $\text{Bi}_2\text{O}_3$ -coated  $\text{LiMn}_{1.42}\text{Ni}_{0.42}\text{Co}_{0.16}\text{O}_4$ . In addition, the microstructure of the surface modification layer plays an important role in determining the electrochemical performances of the active material. Some experimental results indicate that the surface modifications neither change the bulk structure nor cause any change in the cation disorder of the spinel sample. In addition, electrolyte is easy to decompose on the surface of the 5 V spinel cathodes because of the higher operating voltage, resulting in the formation of thick SEI layers. The  $\text{Al}_2\text{O}_3$  coating is the most effective in suppressing of the development of the SEI layer. Thin SEI layer allow lithium-ion conduction. Figure 8 shows the TEM images and rate capabilities of 2 wt.%  $\text{Al}_2\text{O}_3$ -coated  $\text{LiMn}_{1.42}\text{Ni}_{0.42}\text{Co}_{0.16}\text{O}_4$ .

Although the coating method has been approved an effective way to improve cycle performance, it is not much in favor of high rate properties because these inorganic coating layers are not good conductor and there are extra resistance for lithium ion to insert into cathodes. To obtain good electrochemical properties for  $\text{LiNi}_{0.5}\text{Mn}_{1.5}\text{O}_4$ , the microstructure of the surface modification layer conductive to insertion/deinsertion of Li must be constructed.

#### Fabricating advanced Li-ion batteries

The 5-V material  $\text{LiNi}_{0.5}\text{Mn}_{1.5}\text{O}_4$  has also been considered to apply in new lithium-ion battery system. The  $\text{LiNi}_{0.5}\text{Mn}_{1.5}\text{O}_4/\text{Li}_4\text{Ti}_5\text{O}_{12}$  (LNMO/LTO) cell is a good example [142–151]. Its operating voltage is around 3 V, which can avoid PC and some additives decomposing reductively that takes place at higher voltage. The  $\text{Li}_4\text{Ti}_5\text{O}_{12}$  displays excellent reversibility and structural stability as a zero-strain insertion material in the charge–discharge process [152, 153]. So lithium-ion battery with  $\text{Li}_4\text{Ti}_5\text{O}_{12}$  as anode and  $\text{LiNi}_{0.5}\text{Mn}_{1.5}\text{O}_4$  as cathode can exhibit good properties in cycling performance and thermal stability. Xiang [142] reported that the 3 V  $\text{LiNi}_{0.5}\text{Mn}_{1.5}\text{O}_4/\text{Li}_4\text{Ti}_5\text{O}_{12}$  lithium-ion battery with electrolyte (1 M  $\text{LiPF}_6/\text{EC} + \text{DMC}$  (1:1)) exhibited perfect cycling performance. A LTO-limited cell showed high capacity retention of 85% after 2,900 cycles, which is shown in Fig. 9. Although the new system displayed excellent cycle ability, the testing current was  $0.2 \text{ mA cm}^{-2}$ . Cycle ability at high current rates should be explored and improved for this LNMO/LTO system. In addition, Arrebola [154] have tried to combine  $\text{LiNi}_{0.5}\text{Mn}_{1.5}\text{O}_4$  spinel and Si nanoparticles to fabricate new Li-ion batteries. Because Si composite could deliver capacities as high as 3,850 (with super P) and 4,300 (with

MCMC)  $\text{mAh g}^{-1}$ , this  $\text{LiNi}_{0.5}\text{Mn}_{1.5}\text{O}_4/\text{Si}$  cell was expected to have higher capacity. At present, the battery could deliver a capacity of around 1,000  $\text{mAh g}^{-1}$  after 30 cycles with good cycling properties. Xia [155] reported the electrochemical properties of  $\text{LiNi}_{0.5}\text{Mn}_{1.5}\text{O}_4/(\text{Cu}-\text{Sn})$  cell which has a working voltage of 4.0 V.

The high-voltage material gives room for replacement of carbon anodes with anode materials like  $\text{Li}_4\text{Ti}_5\text{O}_{12}$ , which suffers less from SEI formation, is safer and shows higher rate capabilities. So the batteries  $\text{LiNi}_{0.5}\text{Mn}_{1.5}\text{O}_4/\text{Li}_4\text{Ti}_5\text{O}_{12}$  are very promising. Combining  $\text{LiNi}_{0.5}\text{Mn}_{1.5}\text{O}_4$  with other anode materials, appropriate mass ratio of cathode and anode should be observed due to their different theoretical capacities.

#### Conclusions

Spinel  $\text{LiNi}_{0.5}\text{Mn}_{1.5}\text{O}_4$  is a promising cathode material for lithium-ion battery not only because it is inexpensive and environmentally benign but also its discharge charge plateau can reach 4.7 V which is much higher than other cathode materials. The spinel  $\text{LiNi}_{0.5}\text{Mn}_{1.5}\text{O}_4$  has two possible structures, i.e., face-centered spinel ( $Fd3m$ ) and primitive simple cubic crystal ( $P4_332$ ). The Ni and Mn ions are ordered regularly in  $P4_332$  structure. The spinel with  $Fd3m$  structure exhibits better cycling performance than spinel with  $P4_332$  structure at high rates. The microstructure and surface are the key factors affecting its electrochemical properties. Doping element like Ru could make crystal lattice enlarge and lithium ion locate at octahedral sites rather than tetrahedral site, which is in favor of Li insertion/deinsertion. Making surface modification such as coating  $\text{Al}_2\text{O}_3$  on the surface of  $\text{LiNi}_{0.5}\text{Mn}_{1.5}\text{O}_4$ , can not only protect electrode materials from attacking of HF which generates from electrolyte decomposing, but also suppress the development of the SEI layer. This helps to improve the electrochemical properties of spinel  $\text{LiNi}_{0.5}\text{Mn}_{1.5}\text{O}_4$ . The Li insertion/deinsertion is affected by particle morphology and size which depend on synthesis methods as well. Nanomaterials can lead to higher charge/discharge rates. New lithium-ion battery system can be put into practice when combining  $\text{LiNi}_{0.5}\text{Mn}_{1.5}\text{O}_4$  and other anode materials such as  $\text{Li}_4\text{Ti}_5\text{O}_{12}$ . These systems have exhibited excellent electrochemical properties.

#### References

1. Winter M, Brodd J (2004) Chem Rev 104:4254–4259
2. Lithium Ion technical handbook (2009) Gold Peak Industries Ltd. Taiwan
3. Hitachi Maxell KK (1988) Patent JP63211565-A

4. Nagaurat, Yokokawa M, Hashimoto T (1988) Patent GB2196785-A
5. Padhi AK, Nanjundaswamy KS, Goodenough JB (1997) *J Electrochem Soc* 14:1188–1194
6. Lithium Ion Batteries. [http://en.wikipedia.org/wiki/Lithium-ion\\_battery](http://en.wikipedia.org/wiki/Lithium-ion_battery). Accessed 28 February 2010
7. Walter AVS, Scrosati B (2002) *Advances in lithium-ion batteries*. Kluwer Academic/Plenum, New York
8. Nazri GA (2008) *Lithium ion battery science and technology*. Springer, USA
9. Patoux S, Daniel L, Bourbon C, Lignier H, Pagano C, Cras FL, Jouanneau S, Martinet S (2009) *J Power Sources* 189:344–352
10. Patoux S, Bourbon C, Le Cars (2007) Patent FUS2007292760-A1
11. Amine K, Tukamoto H, Yasuda H, Fujita Y (1996) *J Electrochem Soc* 143:1607–1613
12. Strobel P, Palos AI, Anne M, Le Cras F (2000) *J Mater Chem* 10:429–436
13. Morales J, Sanchez L, Tirado JL (1998) *J Solid State Electrochem* 2:420–426
14. Wagemaker M, Ooms FGB, Kelder EM, Schoonman J, Kearley GJ, Mulder FM (2004) *J Am Chem Soc* 126:13526–13533
15. Gryffroy D, Vandenberghe RE, Legrand E (1991) *Mater Sci Forum* 79–82:785–790
16. Ooms FGB, Wagemaker M, van Well AA, Mulder FM, Kelder EM, Schoonman J (2002) *J Appl Phys A* 74:S1089–S1091
17. Kim JH, Myung ST, Yoon CS, Kang SG, Sun YK (2004) *Chem Mater* 16:906–914
18. Amdouni N, Zaghib K, Gendron F, Mauger A, Julien CM (2007) *J Magn Magn Mater* 309:100–105
19. Zhong QM, Bonakdarpour A, Zhang MJ, Gao Y, Dahn JR (1997) *J Electrochem Soc* 144:205–213
20. Sigala C, Guyomard D, Verbaere A, Piffard Y, Tournoux M (1995) *Solid State Ionics* 81:167–170
21. Yang SH, Middaugh RL (2001) *Solid State Ionics* 139:13–25
22. Kawai H, Nagata M, Tukamoto H, West AR (1999) *J Power Sources* 81–82:67–72
23. Ein-Eli Y, Lu SH, Rzeznik MA (2004) *J Electrochem Soc* 145:3383–3386
24. Ein-Eli Y, Howard WF, Lu SH, Mukerjee S, McBreen J, Vaughey JT, Thackeray MM (1998) *J Electrochem Soc* 145:1238–1244
25. Biskup N, Martinez JL, de Dompablo MEAY, Diaz-Carrasco P, Morales J (2006) *J Appl Phys* 100:093908
26. Shigemura H, Tabuchi M, Kobayashi H, Sakaebe H, Hirano A, Kageyama H (2002) *J Mater Chem* 12:1882–1891
27. Oikawa K, Kamiyama T, Izumi F, Nakazato D, Ikuta H, Wakihara M (1999) *J Solid State Chem* 146:322–328
28. Sigala C, Verbaere A, Mansot JL, Guyomard D, Piffard Y, Tournoux M (1997) *J Solid State Chem* 132:372–381
29. Obrovac MN, Gao Y, Dahn JR (1998) *Phys Rev B Condens Matter* 57:5728–5733
30. Aklalouch M, Amarilla JM, Rojas RM, Saadouni I, Rojo JM (2008) *J Power Sources* 185:501–511
31. Shigemura H, Sakaebe H, Kageyama H, Kobayashi H, West AR, Kanno R, Morimoto S, Nasu S, Tabuchi M (2001) *J Electrochem Soc* 148:A730–A736
32. Amine K, Tukamoto H, Yasuda H, Fujita Y (1997) *J Power Sources* 68:604–608
33. Eftekhari A (2004) *J Power Sources* 132:240–243
34. Song D, Ikuta H, Uchida T, Wakihara M (1999) *Solid State Ionics* 117:151–156
35. Kim JS, Vaughey JT, Johnson CS, Thackeray MM (2003) *J Electrochem Soc* 150:A1498–A1502
36. Lee YJ, Park SH, Eng C, Parise JB, Grey CP (2005) *Chem Mater* 14:194–205
37. Shin Y, Manthiram A (2003) *Electrochim Acta* 48:3583–3592
38. Gao Y, Myrtle K, Zhang MJ, Reimers JN, Dahn JR (1996) *Phys Rev B Condens Matter* 54:16670–16675
39. Ohzuku T, Takeda S, Iwanaga M (1999) *J Power Sources* 81–82:90–94
40. Terada Y, Yasaka K, Nishikawa F, Konishi T, Yoshio M, Nakai I (2001) *J Solid State Chem* 156:286–291
41. Ariyoshi K, Iwakoshi Y, Nakayama N, Ohzuku T (2004) *J Electrochem Soc* 151:A296–A303
42. Idemoto Y, Narai H, Koura N (2003) *J Power Sources* 119–121:125–129
43. Fang HS, Wang ZX, Li XH, Guo HJ, Peng WJ (2006) *J Power Sources* 153:174–176
44. Fang HS, Wang ZX, Li XH, Guo HJ, Peng WJ (2006) *Mater Lett* 60:1273–1275
45. Chen ZY, Ji S, Linkov V, Zhang JL, Zhu W (2009) *J Power Sources* 189:507–510
46. Liu GQ, Qi L, Wen L (2006) *Rare Met Mater Eng* 35:299–302
47. Ji Y, Wang ZX, Yin ZL, Guo HJ, Peng WJ, Li XH (2007) *Chin J Inorg Chem* 23:597–601
48. Qiu W, Li T, Zhao H, Liu J (2008) Patent CN1321881-C
49. Chen ZY, Ji S, Zhu HL, Pasupathi S, Bladergroen B, Linkov V (2008) *South African Journal of Chemistry-Suid-Afrikaanse Tydskrif Vir Chemie* 61:157–161
50. Wang Z, Li X, Peng W, Yuan R, Jiang X (2008) Patent CN101148263-A
51. Fang HS, Li LP, Li GS (2007) *Chin J Inorg Chem* 167:223–227
52. Takahashi Y, Sasaoka H, Kuzuo R, Kijima N, Akimoto J (2006) *Electrochem Solid-State Lett* 9:A203–A206
53. Wang ZX, Fang HS, Yin ZL, Li XH, Guo HJ, Peng WJ (2006) *J Cent S Univ Tech* 15:1429–1432
54. Chen ZY, Xiao J, Zhu HL, Liu YX (2005) *Chin J Inorg Chem* 21:1417–1421
55. Fang HS, Wang ZX, Li XH, Yin ZL, Guo HJ, Peng WJ (2006) *Chin J Inorg Chem* 22:311–315
56. Zhang B, Wang ZX, Guo HJ (2007) *Trans Nonferrous Met Soc China* 17:287–290
57. Ohzuku T, Ariyoshi K, Yamamoto S (2002) *J Ceram Soc Jpn* 110:501–505
58. Sun Q, Wang ZX, Li XH, Guo HJ, Peng WJ (2007) *Trans Nonferrous Met Soc China* 17:S917–S922
59. Xiao J, Zeng LY, Chen ZY, Zhao H, Peng ZD (2006) *Chin J Inorg Chem* 22:685–690
60. Fan YK, Wang JM, Ye XB, Zhang JQ (2007) *Mater Chem Phys* 103:19–23
61. Liu GQ, Wang YJ, Lu Q (2005) *Electrochim Acta* 50:1965–1968
62. Xiao LF, Zhao YQ, Yang YY, Ai XP, Yang HX, Cao YL (2008) *J Solid State Electrochem* 12:687–691
63. Yu LH, Cao YL, Yang HX, Ai XP (2006) *J Solid State Electrochem* 10:283–287
64. Yi TF, Zhu YR (2008) *Electrochim Acta* 53:3120–3126
65. Yi TF, Hu XG (2007) *J Power Sources* 167:185–191
66. Fu LJ, Liu H, Li C, Wu YP, Rahm E, Holze R, Wu HQ (2005) *Prog Mater Sci* 50:881–928
67. Liu H, Wu YP, Rahm E, Holze R, Wu HQ (2004) *J Solid State Electrochem* 8:450–466
68. Yi TF, Li CY, Zhu YR, Shu J, Zhu RS (2009) *J Solid State Electrochem* 13:913–919
69. Xu HY, Xie S, Ding N, Liu BL, Shang Y, Chen CH (2006) *Electrochim Acta* 51:4352–4357
70. Lazarraga MG, Pascual L, Gadjov H, Kovacheva D, Petrov K, Amarilla JM, Rojas RM, Martin-Luengo MA, Rojo JM (2004) *J Mater Chem* 14:1640–1647
71. Wu HM, Tu JP, Chen XT, Shi DQ, Zhao XB, Cao GS (2006) *Electrochim Acta* 51:4148–4152
72. Kovacheva D, Markovsky B, Salitra G, Talyosef Y, Gorova M, Aurbach D (2005) *Electrochim Acta* 50:5553–5560
73. Arrebola JC, Caballero A, Hernan L, Morales J (2005) *Electrochem Solid-State Lett* 8:A641–A645

74. Wen L, Lu Q, Xu GX (2006) *Electrochim Acta* 51:4388–4392
75. Kim JH, Myung ST, Sun YK (2004) *Electrochim Acta* 49:219–227
76. Amarilla JM, Rojas RM, Pico F, Pascual L, Petrov K, Kovachev D (2007) *J Power Sources* 174:1212–1217
77. Caballero A, Cruz M, Hernan L, Melero M, Morales J (2005) *J Electrochem Soc* 152:A552–A559
78. Arrebola JC, Caballero A, Hernán L, Morales J (2008) *Eur J Inorg Chem* 21:3295–3302
79. Kunduraci M, Amatucci GG (2008) *Electrochim Acta* 53:4193–4199
80. Xia H, Lu L, Lai MO (2009) *Electrochim Acta* 54:5986–5991
81. Caballero A, Hernan L, Melero M, Morales J, Moreno R, Ferrari B (2006) *J Power Sources* 158:583–590
82. Arrebola JC, Caballero A, Hernan L, Melero M, Morales J, Castellon ER (2006) *J Power Sources* 162:606–613
83. Zhang L, Lv XY, Wen YX, Wang F, Su HF (2009) *J Alloys Compd* 480:802–805
84. Zhao ZQ, Ma JF, Tian H, Xie LJ, Zhou J, Wu PW, Wang YG, Tao JT, Zhu XY (2005) *J Am Ceram Soc* 88:3549–3552
85. Xia H, Meng YS, Lu L, Ceder G (2007) *J Electrochem Soc* 154:A737–A743
86. Li DC, Ito A, Kobayakawa K, Noguchi H, Sato Y (2007) *Electrochim Acta* 52:1919–1924
87. He ZQ, Xiong LZ, Wu XM, Liu WP, Chen S, Huang KL (2007) *Chin J Inorg Chem* 23:875–878
88. Takahashi K, Saitoh M, Sano M, Fujita M, Kifune K (2004) *J Electrochem Soc* 151:A173–A177
89. Kojima M, Mukoyama I, Myoujin K, Kodera T, Ogihara T (2009) *Electroceramics in Japan XI* 388:85–88
90. Mukoyama I, Myoujin K, Nakamura T, Ozawa H, Ogihara T, Uede M (2007) *Electroceramics in Japan X* 350:191–194
91. Raja MW, Mahanty S, Basu RN (2009) *Solid State Ionics* 180:1261–1266
92. Yamada M, Dongying B, Kodera T, Myoujin K, Ogihara T (2009) *J Ceram Soc Jpn* 117:1017–1020
93. Fan WF, Qu MZ, Peng GC, Yu ZL (2009) *Chin J Inorg Chem* 25:124–128
94. Amatucci GG, Schmutz CN, Bylr A, Siala C, Gozdz AS, Larcher D, Tarascon JM (1997) *J Power Sources* 69:11–25
95. Xia Y, Okada M, Nagano M, Yoshio MJ (1997) *Electrochem Soc Ser* 97:494–503
96. Sun YK, Kim DW, Choi YM (1999) *J Power Sources* 79:231–237
97. Markovsky B, Talyossef Y, Salitra G, Aurbach D, Kim HJ, Choi S (2004) *Electrochem Commun* 6:821–826
98. Yamane H, Inoue T, Fujita M, Sano M (2001) *J Power Sources* 99:60–65
99. Arrebola JC, Caballero A, Hernán L, Morales J (2001) *J Power Sources* 195:4278–4284
100. Sun YK, Hong KJ, Prakash J, Amine K (2002) *Electrochem Commun* 4:344–348
101. Arico AS, Bruce P, Scrosati B, Tarascon JM, Schalkwijk WV (2005) *Nanostruct Mater* 4:366–377
102. Bruce P, Scrosati B, Tarascon JM (2008) *Angew Chem Int Ed* 47:2930–2946
103. Talyosef Y, Markovsky B, Lavi R, Salitra G, Aurbach D (2007) *J Electrochem Soc* 154:A682–A691
104. Lafont U, Locati C, Kelder EM (2006) *Solid State Ionics* 177:3023–3029
105. Lafont U, Locati C, Borghols WJH, Łasinska A, Dygas J, Chadwick AV (2009) *J Power Sources* 189:179–184
106. Thirunakaran R, Sivashanmugam A, Gopukumar S, Dunnill CW, Gregory DH (2008) *Mater Res Bull* 43:2119–2129
107. Kunduraci M, Amatucci GG (2006) *J Electrochem Soc* 153:A1345–A1352
108. Shaju KM, Bruce PG (2008) *Dalton Trans* 40:5471–5475
109. Arrebola JC, Caballero A, Cruz M, Hernán L, Morales J, Castellón ER (2006) *Adv Funct Mater* 16:1904–1911
110. Kunduraci M, Al-Sharab JF, Amatucci GG (2006) *Chem Mater* 18:3585–3592
111. Leon B, Lloris JM, Vicente CP, Tirado JL (2006) *Electrochem Solid-State Lett* 9:A96–A100
112. Alcantara R, Jaraba M, Lavela P, Lloris JM, Vicente CP, Tirado JL (2005) *J Electrochem Soc* 152:A13–A18
113. Liu J, Manthiram A (2009) *J Phys Chem C* 113:15073–15079
114. Eli YE, Vaughey JT, Thackeray MM, Mukerjee S, Yang XQ, McBreenc J (1999) *J Electrochem Soc* 146:908–913
115. Alcantara R, Jaraba M, Lavela P, Tirado JL (2004) *J Electrochem Soc* 151:A53–A58
116. Ito A, Li D, Lee Y, Kobayakawa K, Sato Y (2008) *J Power Sources* 185:1429–1433
117. Kim JH, Myung ST, Yoon CS, Oh IH, Sun YK (2004) *J Electrochem Soc* 151:A1911–A1918
118. Liu GQ, Yuan WS, Liu GY, Tian YW (2009) *J Alloys Compd* 484:567–569
119. Alcantara R, Jaraba M, Lavela P, Tirado JL, Biensan P, Peres JP (2003) *Chem Mater* 15:2376–2382
120. Park SB, Eom WS, Cho WII, Jang H (2006) *J Power Sources* 159:679–684
121. Aklalouchb M, Amarilla JM, Roja RM, Saadoune I, Rojo JM (2008) *J Power Sources* 185:501–511
122. Hong KJ, Sun YK (2002) *J Power Sources* 109:427–430
123. Liu GQ, Xie HW, Liu LY, Kang XX, Tian YW, Zhai YC (2007) *Mater Res Bull* 42:1955–1961
124. Aklalouch M, Rojas RM, Rojo JM, Saadoune I, Amarilla JM (2009) *Electrochim Acta* 54:7542–7550
125. Ooms FGB, Kelder EM, Schoonman J, Wagemaker M, Mulder FM (2002) *Solid State Ionics* 152–153:143–153
126. Liu J, Manthiram A (2009) *J Electrochem Soc* 156:A66–A72
127. Wang HL, Xia H, Lai MO, Lu L (2009) *Electrochem Commun* 11:1539–1542
128. Oh SW, Park SH, Kim JH, Bae YC, Sun YK (2006) *J Power Sources* 157:464–470
129. Xu XX, Yang J, Wang YQ, Wang JL (2007) *J Power Sources* 174:1113–1116
130. Du GD, NuLi Y, Yang J, Wang JL (2008) *Mater Res Bull* 43:3607–3613
131. Liu J, Manthiram A (2009) *J Electrochem Soc* 156:A833–A838
132. Liu J, Manthiram A (2009) *J Electrochem Soc* 156:S13–S13
133. Liu J, Manthiram A (2009) *Chem Mater* 21:1695–1707
134. Sun YK, Lee YS, Yoshio M, Amine K (2002) *Electrochem Solid-State Lett* 5:A99–A102
135. Sun YK, Yoon CS, Oh IH (2003) *Electrochim Acta* 48:503–506
136. Sun YK, Lee YS, Yoshio M, Amine K (2003) *J Electrochem Soc* 150:L11–L11
137. Kobayashi Y, Miyashiro H, Takei K, Shigemura H, Tabuchi M, Kageyama H, Iwahori T (2003) *J Electrochem Soc* 150:A1577–A1582
138. Fan Y, Wang J, Tang Z, He W, Zhang J (2007) *Electrochim Acta* 52:3870–3875
139. Alcantara R, Jaraba M, Lavela P, Tirado JL (2004) *J Electrochem Soc* 151:187–192
140. Arrebola J, Caballero A, Hernan L, Morales J, Castellon ER, Barrado JRR (2007) *J Electrochem Soc* 154:A178–A184
141. Arrebola J, Caballero A, Hernan L, Morales J, Castellon ER (2005) *Electrochem Solid-State Lett* 8:A303–A307
142. Xiang HF, Zhang X, Jin QY, Zhang CP, Chen CH, Ge XW (2008) *J Power Sources* 183:355–360
143. Xiang HF, Jin QY, Wang R, Chen CH, Ge XW (2008) *J Power Sources* 179:351–356

144. Ariyoshi K, Yamamoto S, Ohzuku T (2003) *J Power Sources* 119:959–963
145. Wu HM, Belharouak I, Deng H, Abouimrane A, Sun YK, Amine K (2009) *J Electrochem Soc* 156:A1047–A1050
146. Imazaki M, Ariyoshi K, Ohzuku T (2009) *J Electrochem Soc* 156:A780–A786
147. Amazutsumi T, Ariyoshi K, Okumura K, Ohzuku T (2007) *Electrochemistry* 75:867–872
148. Ariyoshi K, Yamatoa R, Makimura Y, Amazutsumi T, Maeda Y, Ohzuku T (2008) *Electrochemistry* 76:46–54
149. Ohzuku T, Ariyoshi K, Yamamoto S, Makimura Y (2001) *Chem Lett* 12:1270–1271
150. Maeda Y, Ariyoshi K, Kawai T, Sekiya T, Ohzuku T (2009) *J Ceram Soc Jpn* 117:1216–1220
151. Niu SJ, Chen M, Jin JM, Sun Y (2007) *Electronic Components and Materials* 26:49–52, in Chinese
152. Zaghbi K, Simoneau M, Armand M, Gauthier M (1999) *J Power Sources* 81:300–305
153. Zaghbi K, Armand M, Gauthier M (1998) *J Electrochem Soc* 145:3135–3140
154. Arrebola JC, Caballero A, Gómez-Cámer JL, Hernán L, Morales J, Sánchez L (2009) *Electrochem Commun* 11:1061–1064
155. Xia YY, Sakai T, Fujieda T, Wada M, Yoshinaga H (2001) *Electrochem Solid-State Lett* 4:A9–A11